Role of H_2O in the thermal annealing of the E'_γ center in amorphous silicon dioxide

Laura Nuccio,* Simonpietro Agnello, and Roberto Boscaino
Dipartimento di Scienze Fisiche ed Astronomiche, Università di Palermo, Via Archirafi 36, I-90123 Palermo, Italy
(Received 23 December 2008; revised manuscript received 16 February 2009; published 30 March 2009)

The model for the annealing of a radiation-induced point defect in silica, the E'_γ center, is identified in the temperature range (150–550) °C. Thermal treatments in controlled atmospheres of water vapor, oxygen, or helium of irradiated amorphous silicon dioxide are carried out. Direct experimental evidences that the annealing of the E'_γ center is caused by a reaction with diffusing water molecules are found. A rate equation system describing this annealing process is inferred, and its solutions are compared with experimental data to obtain quantitative information. In particular, the activation energy, its distribution and the way the latter is modified by thermal treatments are derived. The process was also established to be reaction limited. The mean activation energy value for the annealing process of the E'_γ center due to water is found to be 1.23 eV.

DOI: 10.1103/PhysRevB.79.125205 PACS number(s): 61.82.Ms, 66.30.jj, 81.05.Kf, 82.20.Pm

I. INTRODUCTION

The interest toward thermal treatments of amorphous silicon dioxide and the role played by small molecules as water can be ascribed to both technological and basic reasons.[1–5] In fact, in the industrial manufacturing procedures of many *a*-SiO_2 based devices, thermal annealing is often employed to relax stresses induced during the production. Thermal treatments can be also used to cancel radiation effects. In particular, a change in the concentrations of radiation-induced point defects can be determined by heating an irradiated sample above specific threshold temperatures that depend on the defect itself, the material, and the treatment conditions. This phenomenon is of particular interest because of the highly detrimental effects due to the presence of point defects. On the other hand thermal treatments can also be a useful tool for the study of the properties of point defects.

In this contest many results on the effects of thermal treatments on the E'_γ center[6] ($\equiv Si^\bullet$, where the symbol $\equiv$ indicates three bonds with oxygen atoms and $\bullet$ an unpaired electron) were reported[1–4,7–9] due to the importance of this defect and its ubiquitous presence in irradiated silica. However a complex scenario results from these previous studies, as described in the following.

Isochronal annealing of E'_γ, peroxy radical ($\equiv$Si-O-O$^\bullet$, named as POR hereafter) and nonbridging oxygen hole centers ($\equiv$Si-O$^\bullet$, also called NBOHC)[6] in irradiated dry silica were studied by Stapelbroek *et al.*[4] The decay of E'_γ and NBOHC was observed, together with the growth of POR, at temperatures higher than ~150 °C. They hypothesized that the precursor site of POR releases an electron and that the E'_γ center, which is thought to be a hole trapped in an oxygen vacancy, is consequently annealed. Alternatively, basing on the simultaneous one-for-one growth of the peroxy radicals, the same result was later reinterpreted in terms of the reaction of the E'_γ center with diffusing molecular oxygen through the reaction[1,10]

$$\equiv Si^\bullet + O_2 \rightarrow \equiv Si\text{-}O\text{-}O^\bullet. \quad (1)$$

The oxygen involved in this reaction can in fact be available due to radiolytic processes as the energy of γ rays allows the displacement of bounded oxygen atoms that can then dimerize to form O_2.[10]

The annealing of the E'_γ center observed in high OH silica at temperatures higher than ~300 °C was instead attributed to its reaction with diffusing water according to the reaction[3,8]

$$\equiv Si^\bullet + H_2O \rightarrow \equiv SiOH + H. \quad (2)$$

Water molecules were hypothesized to have a radiolytic origin, too, created by the reaction between displaced oxygen atoms and radiolytic hydrogen.[3,8]

Finally, the E'_γ annealing was also observed in oxygen-deficient low-OH samples at temperatures higher than in other materials.[3] Due to the fact that the concentration of molecular species that can diffuse was hypothesized to be very low and that the annealing of the E'_γ center takes place at temperatures higher than in other materials in this case, the authors proposed that the E'_γ annealing in this sample is due to thermal excitation of holes to the valence band or electrons to the conduction band.[3]

In a recent paper, we suggested that a distribution of the activation energies for the process responsible for the annealing of this defect exists.[11] Similar hypothesis had been put forward previously,[8] but they had not been fully clarified. We also suggested that thermal treatments could modify this distribution, affecting the thermal response of a given material depending on its previous thermal history.[11] Notwithstanding the great interest in this annealing process, a general scheme has not been established yet. Furthermore, some important aspects of this process, as being diffusion or reaction limited, and quantitative information about it need to be clarified.

In this paper we will show the results of an extensive and articulated set of experiments, aiming to give a general description of the thermal annealing process of the E'_γ center. Evidences are found that the annealing of the E'_γ center occurs through processes involving H_2O and that these processes are reaction limited. The activation energy value and the parameters that characterize the distribution are determined by comparing the experimental data with the solutions of the obtained rate equation system describing the process.

II. EXPERIMENTAL DETAILS: SAMPLES AND MEASUREMENTS

The E'_γ center is detected by electron paramagnetic resonance (EPR) measurements. These measurements were carried out at 300 K using a Bruker EMX spectrometer working at 9.8 GHz (X band). The E'_γ center signal was revealed with a microwave power $P=0.8$ μW and a modulation field with peak-to-peak amplitude $B_m=0.01$ mT and frequency $f_m=100$ kHz. These EPR measurement conditions do not distort the EPR line shape and do not induce microwave saturation effects. The concentration of E'_γ centers was estimated by comparing the double integral of the EPR signal of the sample under examination with that of the E'_γ centers in a silica sample whose defect concentration was determined by spin-echo experiments.[12] We have estimated an absolute accuracy of 20% in this procedure; the relative concentrations are affected by a 5% uncertainty. POR and NBOHC are detected by EPR, too, in the same conditions as the E'_γ centers but for a microwave power $P=126$ mW and a modulation field with peak-to-peak amplitude $B_m=0.3$ mT.

Infrared (IR) absorption spectra of the samples were measured using a Bruker Vertex70 Fourier transform infrared (FTIR) spectrophotometer with a spectral resolution of 1 cm^{-1}. The absorption band at 3670 cm^{-1} was used to detect the presence of OH groups. The uncertainty in the band amplitude value is 1%. The concentration of OH groups was estimated using the Lambert-Beer law $A=\epsilon Cd$, where A is the absorbance at the band maximum, ϵ is the extinction coefficient,[13] C is the concentration of absorbing species, and d is the path length of absorption.

Raman spectroscopy has been also used to detect interstitial oxygen molecules. In fact, it was shown that the presence of interstitial O_2 causes an infrared PL band at 1272.2 nm excited at 1064 nm, associated to the forbidden transition $a^1\Delta_g \rightarrow X^3\Sigma_g^-$ of the oxygen molecule,[14] to appear in the Raman spectrum of silica samples. The intensity of this PL band is calibrated against the neighboring intrinsic Raman scattering bands of SiO_2 at ~ 1060 cm^{-1} and ~ 1200 cm^{-1} and the oxygen concentration is estimated by comparison in accordance with literature data.[14] Raman spectra were measured using a Bruker RamII Fourier transform spectrometer, with Nd-YAG laser excitation ($\lambda=1064$ nm). The spectral resolution of these measurements was 5 cm^{-1}. The uncertainty on the estimation of the concentration of interstitial oxygen molecules was evaluated to be $\sim 20\%$. All the measurements were carried out at room temperature.

Two different experiments are presented in the following. In the former, three samples of the synthetic dry material Suprasil F300 (supplied by Heraeus) that will be hereafter called F300/H20, F300/He, and F300/O2 were used. The samples are disks 2 mm thick, cut from a cylinder of diameter 6.5 mm, and then optically polished. Preliminary to the experiment, they were γ irradiated at room temperature (^{60}Co source, dose rate of ~ 3 kGy/h), up to a total dose of 1500 kGy, so that the concentrations of a given defect were approximately the same in all the samples. In particular, the E'_γ center concentration was $\sim 6.7\times 10^{16}$ centers/cm^3.

In the second experiment a sample of the synthetic dry material Suprasil 300 (supplied by Heraeus), referred to as S300/An in the following, was used. Its size was $5\times 5\times 1$ mm^3, and its widest surfaces were optically polished. Preliminary to the annealing experiment, it was γ irradiated (^{60}Co source, dose rate of ~ 3 kGy/h) at room temperature up to a total dose of 4000 kGy. The E'_γ center concentration was estimated to be about 7.5×10^{16} centers/cm^3 after the irradiation.

The samples have been subjected to isothermal heat treatments at different temperatures, whose details are described in the following. An isothermal treatment is a series of heat treatments at a fixed temperature and whose duration progressively increases.

The thermal treatments on the Suprasil F300 samples (first experiment) were performed in controlled atmosphere using a Parr reactor. The temperature is measured through a thermocouple and is controlled by means of a digital feedback system. The target temperature can be set with an accuracy of ± 1 °C. The pressure is measured by both a digital and an analogical pressure gauges. High-purity He and O_2 were used, the main impurity being water with a concentration lower than 3 ppm mol. Water vapor was instead generated during the treatments by putting liquid deionized water (resistivity ~ 18.2 MΩ cm) inside the sample chamber. A stainless steel sample holder was used to avoid the sample getting in contact with liquid water. The same sample holder was used in the other treatments, too, to guarantee comparable experimental conditions in all the experiments. At each treatment the sample is inserted into the reactor at room temperature, as the insertion procedure cannot be carried out at higher temperatures. Then, after a heating time of about 2 h that is comparable for all the treatments, the target temperature is reached. At the end of the time length that the sample has to spend at the target temperature, the heater is turned off and, after cooling down to room temperature, the sample is extracted from the reactor to carry out the measurements. It is worth noting that the heating and cooling rates do not play a relevant role in this experiment. In fact, the conclusions are drawn by comparing the effects on the three samples that experienced the same heating and cooling conditions. However, due to their not negligible duration, these conditions could influence eventual quantitative estimation of the annealing rates. For this reason these data were not used to obtain quantitative results. A different experiment that will be described hereafter was performed to this aim using a different system.

The Suprasil 300 (second experiment) was thermally treated in air using an electric furnace whose temperature control is made by a thermocouple and a digital controller. The target temperature can be set with an accuracy of ± 3 °C. At each treatment the sample is inserted into the oven that has previously reached the target temperature, and at the end it is extracted from the oven and brought back to room temperature in air to carry out the measurements. This heating and cooling conditions have been chosen to minimize the time that the sample spends at temperatures different from the target temperature of the treatment.

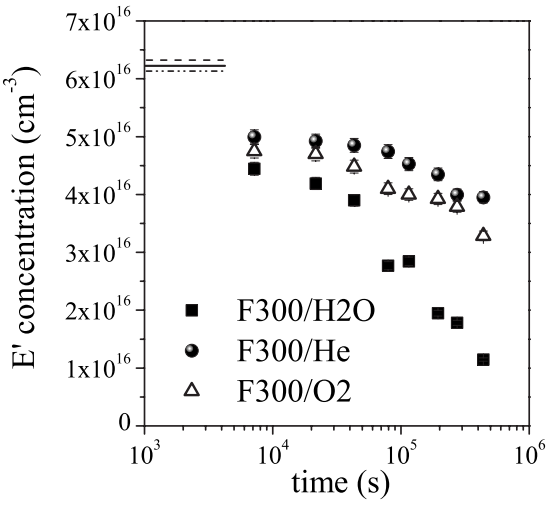

FIG. 1. E'_γ center concentrations as a function of the treatment time at 250 °C in the F300 samples treated in H_2O (squares), He (circles), and O_2 (triangles) atmospheres. Initial concentrations are represented by continuous line (F300/H2O), dashed line (F300/He), and dash-dotted line (F300/O2). Error bars are comparable to the size of points.

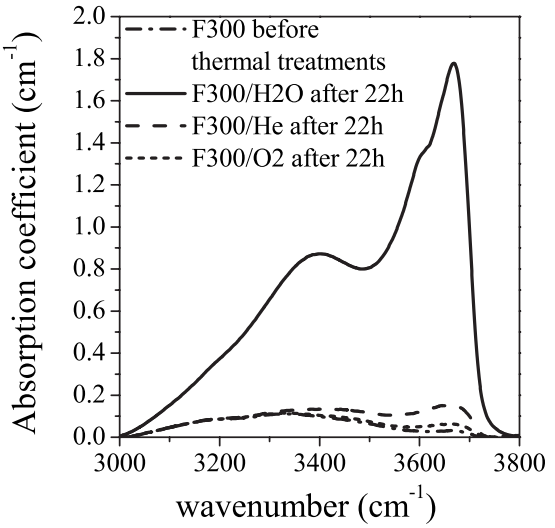

FIG. 2. Infrared absorption spectra of the samples F300/H2O (continuous line), F300/He (dashed line), and F300/O2 (short-dashed line) after 22 h treatments at 250 °C. The dash-dotted line is the spectrum of one of these samples before the thermal treatment.

III. RESULTS AND DISCUSSION

A. Identification of the microscopic mechanism of the annealing of the E'_γ center

The three samples F300/H20, F300/He, and F300/O2 were subjected to isothermal heat treatments at 250 °C and ~35 bar in water, helium, or oxygen atmospheres, respectively. These treatments were performed in the Parr reactor described in Sec. II. The only difference between these three treatments was the treatment atmosphere.

The isothermal annealing curves of E'_γ at a given temperature that represent the defect concentration as a function of the treatment time were obtained. In Fig. 1 a comparison between these curves for the three samples is shown.

The initial concentrations, indicated by lines, are comparable in the three samples. It can be easily observed that almost comparable results are obtained by treating the samples in helium and oxygen atmospheres (circles and triangles in Fig. 1). The annealing rate of E'_γ centers is instead considerably higher in the water vapor treated sample (squares).

The IR absorption spectra of the samples were measured to detect the presence of molecular water and of SiOH groups that should be generated if reaction (2) were effective. In Fig. 2 the IR absorption spectra of the three samples after 22 h treatments are shown, compared to the spectrum of a sample before the thermal treatments (dash-dotted line). The spectra at the other treatment times show the same behavior. The initial concentration of OH groups in the samples, before the thermal treatments, was less than 10^{17} cm^{-3}. It can be observed that the intensity of the OH absorption band at 3670 cm^{-1} in F300/He and F300/O2 is of the same order of magnitude even if it is slightly lower in the F300/O2 ($[OH]_{F300/He}=2.5*10^{17}$ cm^{-3} and $[OH]_{F300/O2}=1.0\times10^{17}$ cm^{-3}). These intensities are much lower than in the F300/H2O ($[OH]_{F300/H2O}=2.6\times10^{18}$ cm^{-3}). The F300/H2O also shows a different spectrum profile. In fact a broad band around 3400 cm^{-1} can be observed, demonstrating that molecular water was absorbed from the atmosphere.[15] Moreover a shoulder on the low wave-number side of the OH absorption band (around 3600 cm^{-1}) is clearly detectable. This contribution to the absorption band is attributed to hydrogen bonded OH groups.[16]

No differences in the Raman spectra of the three samples were observed, apart from the growth in the sample F300/O2 of the photoluminescence absorption band at 1272.2 nm excited at 1064 nm of interstitial molecular oxygen, absent in all the samples before the treatments. An O_2 concentration of ~10^{17} molecules/cm^{-3} was estimated in this sample after the overall treatment.

The initial high and almost comparable decrease in E'_γ concentration in the three samples, already observed after ~7000 s, could be attributed to fast processes (for example reactions with residual hydrogen molecules could be hypothesized[7]) and does not influence the subsequent behaviors.

The experimental evidence of the higher efficiency of the annealing of the E'_γ in the sample treated in water vapor atmosphere leads directly to the conclusion that the microscopic process responsible for this annealing is the diffusion of water molecules and their reaction with the defect. In fact the rate of a bimolecular reaction, as the one between a point defect and a diffusing molecule, increases by increasing the concentrations of reactants.[17] As a consequence, as the initial E'_γ concentration is the same in the three samples, a strong increase in the rate should be observed when increasing the concentration of the molecule responsible for the E'_γ annealing by saturating the treatment atmosphere with it. This effect is indeed observed by treating the sample in water vapor atmosphere and allows us to identify water as the reactive molecule that causes the E'_γ thermal annealing in this experiment. This experimental evidence could also be expected by

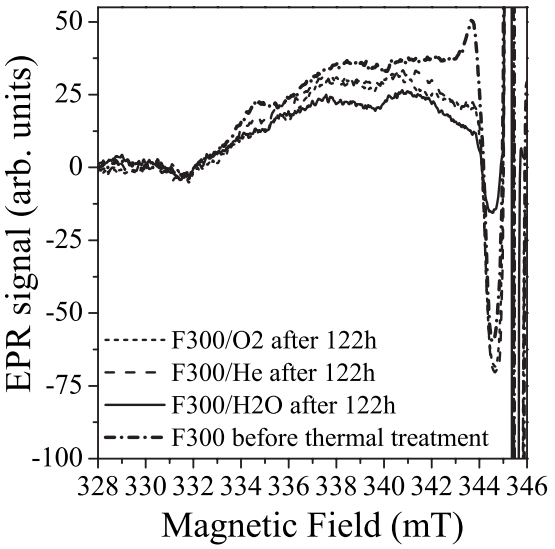

FIG. 3. EPR spectra of NBOHC and POR in the F300/H2O (continuous line), F300/He (dashed line), and F300/O2 (short dashed line) after 122 h treatments at 250 °C. The dash-dotted line is the spectrum of one of these samples before the thermal treatment.

considering that the activation energy for diffusion of water is lower than the one of oxygen, making the diffusion of the former and its ability to reach a defect site more efficient.[18]

Moreover, if the reaction with oxygen (reaction (1)) gave a strong contribution to the E'_γ annealing, an increased number of POR should be observed. In Fig. 3 the EPR spectra of the three samples after 122 h treatments are compared to that of an untreated sample (dash-dotted line). The spectra at different treatment times show the same features. In particular the peak around 335 mT can be considered a fingerprint of the presence of POR, basing on their known principal g values, to computer simulations of their line shapes and to annealing experiments whose effect is to fully anneal the NBOHC but not the POR.[4] No growth of this signal can be observed in any of the three samples.

This evidence proves that the reaction with oxygen does not constitute a significant contribution to the E'_γ annealing. It can be concluded that the E'_γ centers efficiently react with water molecules but not with oxygen. So the main process responsible for the annealing of the E'_γ centers at 250 °C is their reaction with water molecules.

In this framework, the E'_γ annealing observed in samples treated in different atmospheres can be attributed to the water molecules already present in the material due to production technique, irradiation, or, for thermal treatments performed in air, also absorbed from the atmosphere.

The slightly higher efficiency of E'_γ annealing in F300/O2 with respect to F300/He deserves to be commented. A first reason for this behavior could be the initial slightly lower E'_γ concentration in the F300/O2 with respect to F300/He that can be reflected on the following annealing. However another reason can be put forward. The above reported experimental evidence of water being the main responsible for the E'_γ annealing does not exclude a small contribution of the previously suggested reaction of E'_γ with oxygen.[1,10] The latter could in fact be entirely negligible in normal or water excess treatment conditions but can give a small detectable contribution when the treatment atmosphere is saturated by oxygen. In this latter case, in fact, the rate of annealing by oxygen could be enhanced due to its greater concentration in the treatment atmosphere; as a consequence this process could become detectable. This could be the case for the sample F300/O2, in which oxygen loading took place during the thermal treatment. However, the above-mentioned lack of growth of the EPR signal of POR indicates that reaction (1) does not give significant contributions to the E'_γ annealing even in oxygen excess treatment conditions.

Once proved that the annealing of E'_γ centers is due to their reaction with water molecules, the OH concentration should be expected to feature an increase corresponding to the decrease in E'_γ concentration (see reaction (2)). The lowest induced OH concentrations, those in F300/He and F300/O2, are 2.5×10^{17} and 1.0×10^{17} cm^{-3}, respectively. These OH concentrations are higher than the E'_γ concentration decrease in these two samples that are $\sim2\times10^{16}$ cm^{-3} and $\sim2.4\times10^{16}$ cm^{-3}, respectively (see Fig. 1). The same behavior is observed at the other treatment times. These data are compatible with the proposed reaction (2), but a direct correlation between the generated SiOH groups and the annealed E'_γ centers cannot be found because of the existence of other, already known, phenomena that generate SiOH, too.[18–21] In particular, the intense OH absorption in the F300/H2O sample can be explained by a main contribution due to OH groups generated through reaction of the silica matrix with the absorbed water molecules.[18,20,21] The induced absorption in the F300/He and F300/O2 can be instead explained in terms of the processes discussed in a previous work about the generation of silanol groups in dry silica upon thermal treatments probably due to reactions with hydrogen molecules.[19] It can be stated that the observed OH generation is compatible with reaction (2), but the possibility to observe a direct correlation between the annealed E'_γ and the induced OH is prevented by other overriding contributions to the OH generation.

Concluding, we individuated the main microscopic mechanisms for the annealing of the E'_γ center at 250 °C among those proposed in literature. This defect is annealed by reacting with water molecules according to reaction (2).

B. Quantitative analysis of the annealing process

In this section a set of experimental data will be presented to characterize the properties of reaction (2). In particular, the treatment temperatures are extended to a wider range, aiming to verify the reliability of reaction (2) as annealing mechanism for the E'_γ centers at temperatures different from 250 °C. Moreover, these treatments are performed in air because this is a more common and so more interesting condition and because this choice allows to drastically reduce the heating and cooling times, making them negligible with respect to the treatment length and allowing a quantitative analysis on the annealing rates.

The sample S300/An was subjected to a sequence of isothermal heat treatments at 80, 150, 300, and 550 °C in air.

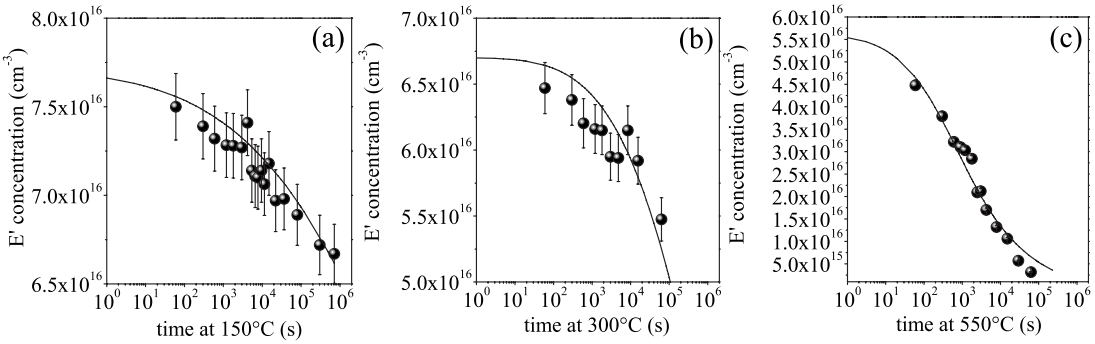

FIG. 4. Concentration of E'_γ (symbols) as a function of the treatment time at (a) 150, (b) 300, and (c) 550 °C as detected in the sample S300/An. Lines are solutions of the rate Eq. (11). See text.

The overall treatment at 80 °C lasted 12 600 s and induced no significant changes in the concentrations of defects. The other annealing curves for the E'_γ center in the sample S300/An are shown in Fig. 4. As expected, the annealing process becomes more efficient on increasing the temperature.

Reaction 2 was established to be responsible for the annealing of E'_γ centers at 250 °C in the experiments presented in Sec. III A. We will assume it valid at the other temperatures, too, and we will *a posteriori* verify the validity of this assumption. It is evident that further reactions are required to account for the fate of the hydrogen atom generated by reaction (2). According to literature data, its dimerization forming H_2 and the reactions of both H and H_2 with the E'_γ have to be taken into account.[22,23] The system of reactions hypothesized taking into account all these processes is

$$E'_\gamma + H_2O \xrightarrow{k_1} \equiv SiOH + H, \tag{3a}$$

$$E'_\gamma + H \xrightarrow{k_2} \equiv SiH, \tag{3b}$$

$$H + H \xrightarrow{k_3} H_2, \tag{3c}$$

$$E'_\gamma + H_2 \xrightarrow{k_4} \equiv SiH + H. \tag{3d}$$

From these reactions a rate equations system can be derived

$$\frac{d[E']}{dt} = -k_1[E'][H_2O] - k_2[E'][H] - k_4[E'][H_2], \tag{4}$$

$$\frac{d[H_2O]}{dt} = -k_1[E'][H_2O], \tag{5}$$

$$\frac{d[H]}{dt} = k_1[E'][H_2O] - k_2[E'][H] - k_3[H]^2 + k_4[E'][H_2], \tag{6}$$

$$\frac{d[H_2]}{dt} = k_3[H]^2 - k_4[E'][H_2], \tag{7}$$

where k_1, k_2, k_3, and k_4 are the rate constants relative to reactions (3). The order of magnitude of these rate constants can be estimated. Reactions (3b) and (3c) are limited by diffusion of atomic hydrogen, and the values of k_2 and k_3 can be calculated, according to the theory for diffusion limited reactions, as

$$k_i = A_i \exp\left(-\frac{E_{ai}}{k_B T}\right) = 4\pi r_{0i} D_{0i} \exp\left(-\frac{E_{ai}}{k_B T}\right), \tag{8}$$

where D_{0i} and E_{ai} are the pre-exponential factor and the activation energy for diffusion, k_B is the Boltzmann's constant, and T is the absolute temperature at which the reactions take place. r_{0i} is the capture radius that represents a distance under which the reaction is supposed to immediately take place, and it is usually considered $\approx 5 \times 10^{-8}$ cm for reactions between point defects and small molecules in silica.[10] The value of k_2 and k_3, calculated at room temperature taking into account this dependence and the typical values of pre-exponential factor and activation energy for atomic hydrogen diffusion,[18] is $k_2 \approx k_3 \approx 6 \times 10^{-14}$ cm^3 s^{-1}. Reaction (3d) is reaction limited, and the values of pre-exponential factor and activation energy are known by literature data.[22] As a consequence k_4 at room temperature can be calculated and the value obtained is $k_4 \approx 1 \times 10^{-20}$ cm^3 s^{-1}. Finally the character of reaction (3a) is not known *a priori*. It can be hypothesized to be diffusion limited. In this case the value of k_1 can be calculated using Eq. (8) and literature values for the pre-exponential factor and activation energy,[8,18] and at room temperature it is $k_1 \approx 2 \times 10^{-26}$ cm^3 s^{-1}. As a consequence it can be concluded that $k_1 \ll k_2$, k_3, k_4, and $k_4 \ll k_2 \approx k_3$. It is worth noticing that even if the hypothesis of reaction (3a) being diffusion limited does not apply, these relations between k_i remain valid. In fact, if reaction (3a) were reaction limited, instead than diffusion limited, the value of k_1 would be even smaller, confirming the above reported relations.

Let us suppose that at the beginning of the process E'_γ and H_2O are present in a comparable amount inside the sample. Then their concentrations start to decrease due to reaction (3a). Atomic hydrogen is instead a *transient product*, as it is

TABLE I. Rate constant values for the annealing of E'_γ and widths of the distributions of activation energy in the sample S300/An treated at 150, 300, and 550 °C, and in the sample I301 (Ref. 11) treated at 300 and 450 °C.

	S300 150 °C	S300 300 °C	S300 550 °C	I301 300 °C	I301 450 °C
k	1.0×10^{-27} cm^3 s^{-1}	7.8×10^{-24} cm^3 s^{-1}	1.6×10^{-20} cm^3 s^{-1}	7.8×10^{-24} cm^3 s^{-1}	1.2×10^{-21} cm^3 s^{-1}
σ_1	0.45 eV	0.28 eV	0.25 eV	0.4 eV	0.25 eV
σ_2	0.4 eV	0.4 eV	0.25 eV	0.4 eV	0.35 eV

slowly (rate constant k_1) produced by reaction (3a) and rapidly (rate constants k_2 and k_3) consumed by reactions (3b) and (3c). Even if it were present in a higher initial concentration, H will be consumed by reactions (3b) and (3c) in a time depending on k_2 and k_3 during which the much slower reaction (3a) is almost *frozen*. Apart from this possible fast transient that could influence the process at short times but not the overall kinetics, H concentration is always much smaller than those of E'_γ and H_2O ($[H]\ll[E'_\gamma],[H_2O]$). Moreover, the dependence on time of its concentration follows the slow changes of $[E'_\gamma]$ and $[H_2O]$ but with the before-mentioned lower concentration.

These considerations lead to the possibility to apply the so-called *steady-state approximation*[17,24]

$$\frac{d[H]}{dt} = k_1[E'][H_2O] - k_2[E'][H] - k_3[H]^2 + k_4[E'][H_2] \sim 0. \tag{9}$$

Analogous considerations can be applied to H_2, whose diffusion is rather faster than that of H_2O, and the steady-state approximation can be applied to it, too,

$$\frac{d[H_2]}{dt} = k_3[H]^2 - k_4[E'][H_2] \sim 0. \tag{10}$$

These approximations allow to eliminate H and H_2 from the rate equations, and the rate equations system reduces to

$$\frac{d[E']}{dt} = 2\frac{d[H_2O]}{dt} = -2k_1[E'][H_2O]. \tag{11}$$

As the approximations made do not depend on the character of reaction (3a), these rate equations are valid in both the cases of diffusion or reaction limited process. As mentioned above, k_1 can be written according to the Arrhenius dependence usually shown by rate constants, $k_1 = A\exp(-\frac{E_a}{k_BT})$, where the pre-exponential factor assumes the form $A = 4\pi r_0 D_0$ in the special case of diffusion limited process [see Eq. (8)].

According to previously reported results,[11] the activation energy values E_a are distributed due to glassy disorder. A convolution of the solutions of Eq. (11) with a statistical distribution was carried out to take into account this phenomenon. A first attempt to describe this disorder effect by means of a Gaussian distribution was made, but the resulting solutions of the rate equations did not satisfactorily describe the experimental data. As a consequence an asymmetric distribution was introduced. It was described as the matching of two half Gaussians having the same mean value E_a and different widths. A half Gaussian describes the distribution at energies lower than E_a and the other one at energies higher than E_a. So two σ were introduced. They were called σ_1 and σ_2 and describe the width on the lower and higher sides, respectively, of E_a.

A comparison between the experimental annealing curves of the E'_γ center in the S300/An sample and the solutions of the rate equations is shown in Fig. 4. As anticipated, in this figure filled symbols represent the observed E'_γ concentration as a function of the treatment time at (a) 150, (b) 300, and (c) 550 °C. Lines are the result of a fitting procedure performed by introducing the asymmetrical statistical distribution for the activation energy mentioned above. The initial values of $[E'_\gamma]$ were the ones measured before each treatment. The water concentration at the beginning of the treatment at 150 °C was set equal to the total amount of water necessary to account for the overall (from 150 to 550 °C) annealing of E'_γ centers. At each following temperature step (300 and 550 °C) this initial $[H_2O]$ value was decreased of a quantity equal to the number of water molecules consumed in the previous ones. The pre-exponential factor for water diffusion D_0 and the capture radius r_0 were set equal to literature values, $D_0 = 1\times10^{-6}$ cm^2 s^{-1} and $r_0 = 5\times10^{-8}$ cm, and were used to calculate A.[8] The activation energy and the widths of its distribution were determined through the fitting procedure. The uncertainties on the activation energy values and on the widths are ±0.01 and ±0.02 eV, respectively.

It can be easily observed that the solutions of the fitting procedure are in reasonable agreement with the experimental data. The rate constants calculated substituting in Eq. (8) the above-mentioned D_0 and r_0 values and the mean E_a values obtained through the fitting are reported in Table I, together with the widths of the distributions of activation energy corresponding to the solutions plotted in Fig. 4.

The reason for reporting k instead than E_a is that single temperature experiments do not allow to obtain the true values for the activation energy and the pre-exponential factor as the E_a value at a fixed temperature depends on the specific values of D_0 and r_0 used to calculate A. Only the widths and k have a direct physical meaning. The *true* values of E_a and A can only be found by comparing data at different temperatures. Our data allow such analysis. In Fig. 5 the Arrhenius plot relative to process (3a) is shown. The $\ln(k)$, calculated using the mean values in Table I, is plotted as a function of the inverse of the absolute temperature. In the same graph the values obtained on a different material that was γ-irradiated and subjected to isothermal heat treatments in normal atmosphere at 300 and 450 °C are also reported for comparison (Infrasil 301, natural dry and supplied by

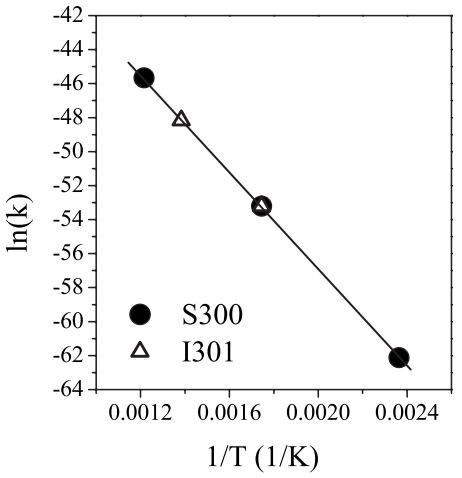

FIG. 5. Arrhenius plot relative to the annealing of the E'_γ centers.

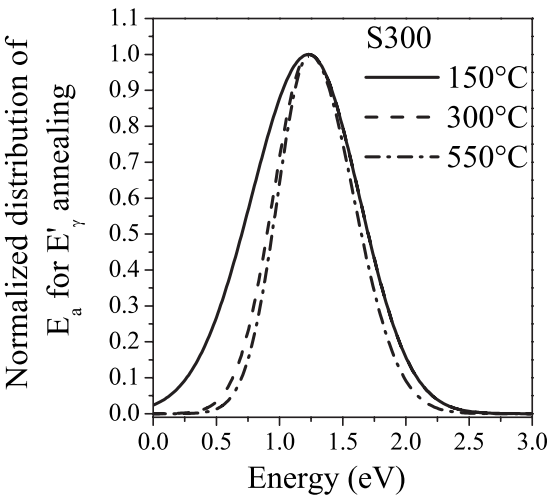

FIG. 6. Distributions of E_a, based on the parameters in Table I for the S300/An sample. Continuous line represents the distribution at 150 °C, dashed line at 300 °C, and dash-dotted line at 550 °C.

Heraeus; data presented in Ref. 11 and not shown here). The k values and the widths for the activation energy distributions in this sample are also shown in Table I. Different symbols correspond to values of k in different samples.

The straight line is a linear fit of the data according to the Arrhenius law. The true values $E_a=1.23$ eV and $A=6.8\times10^{-13}$ cm^3 s^{-1} are found from the linear fit. The same analysis was performed by using the mean values of the activation energies weighted over the statistical distribution, instead than the peak values, to calculate k, and comparable results were obtained.

The fact that all the data can be fit by a single Arrhenius law proves that in all the cases examined the microscopic process is the same. So reaction (3a) is responsible for the annealing of the E'_γ, depending neither on the sample nor on the treatment, in the whole temperature range examined (from 150 to 550 °C). The rate constant for process (3a) can be now calculated using the obtained values for E_a and A.

The value of activation energy obtained is surprisingly similar to the activation energy for the diffusion of molecular oxygen. However, if a diffusion limited reaction with O_2 is hypothesized even if in contrast with the experimental results in Sec. III A, it is worth noticing that the expected rate for such a process should be of the order of 4×10^{-30} cm^3 s^{-1}. This value, calculated at room temperature using literature values of the diffusion activation energy and pre-exponential factor,[25] is higher than the experimental one. The latter, calculated using the obtained values for E_a and A, is in fact of the order of 1×10^{-33} cm^3 s^{-1}. So the reaction could not be a diffusion limited reaction with an oxygen molecule. On the other hand, if a reaction limited reaction with O_2 were considered, there would be no reason why the activation energy of such a reaction limited process should be the same as the activation energy for the diffusion of one of the reactants. This considerations, together with experimental evidence of water being the main responsible for this annealing process shown in Sec. III A, let us conclude that the fact that the obtained value of activation energy for the reaction is comparable to the activation energy for oxygen diffusion has to be considered a coincidence.

The activation energy distributions found deserve attention. A description of these distributions was obtained. In Fig. 6, the distributions of E_a in the sample S300/An at the three different temperatures are shown.

It can be observed that the width of the distribution asymmetrically decreases by progressively increasing the treatment temperature. This result strongly confirms the idea[11] that the sequence of thermal treatments modifies the activation energy distribution for the annealing of point defects. It is found in fact that thermal treatments erode those processes having lower activation energy, evidencing the inhomogeneity of the process.

As mentioned above the rate constant for process (3a), calculated at 300 K using the obtained values for E_a and A, is $k_{\mathrm{exp}}=1\times10^{-33}$ cm^3 s^{-1}. The value expected for diffusion limited processes involving H_2O, calculated considering the literature data of E_a and D_0 for water diffusion [$E_a=0.79$ eV and $D_0=1\times10^{-6}$ cm^2 s^{-1} (Ref. 8)], is $k_{\mathrm{diff}}=2\times10^{-26}$ cm^3 s^{-1}, much higher than the experimental value k_{exp}. This comparison between the experimental value and the value expected for diffusion limited processes makes immediately evident that the theory of diffusion limited processes is not adequate to account for the experimental data. In fact the observed process is slower than expected for a diffusion-limited process. This evidence indicates directly that reaction (3a) is reaction limited.

This fact also means that the distributions of activation energy found are relative to the activation energy for reaction. This latter fact, already guessed basing on qualitative considerations,[11] can be unambiguously stated thanks to the quantitative analysis shown in this section.

IV. CONCLUSIONS

A complete characterization of the annealing processes of the E'_γ center was given in the temperature range (150–550) °C.

The microscopic process was unambiguously identified as a reaction with diffusing water molecules.

The solutions of the rate equations describing this process were compared to the experimental data, and the values of activation energy and the shape of its distribution were obtained. A quantitative estimation of the changes induced in the activation energy distribution by thermal treatments was obtained too, evidencing that an asymmetric shrinkage occurs. It was also concluded that this annealing process is reaction limited, with mean activation energy value $E_a = 1.23$ eV.

ACKNOWLEDGMENTS

We thank Fabrizio Messina and the other people of the LAMP laboratory of Palermo for useful discussions and comments. E. Calderaro and A. Parlato are acknowledged for taking care of gamma irradiation at the IGS-3 irradiator at the Department of Nuclear Engineering of the University of Palermo. Partial financial support by POR Sicilia 2000/2006 Misura 3.15-Sottoazione C and technical assistance by G. Napoli and G. Tricomi are acknowledged.

*laura.nuccio@fisica.unipa.it

[1] L. Zhang, V. A. Mashkov, and R. G. Leisure, Phys. Rev. Lett. **74**, 1605 (1995).
[2] J. W. Lee, M. Tomozawa, and R. K. MacCrone, J. Non-Cryst. Solids **354**, 1509 (2008).
[3] D. L. Griscom, Nucl. Instrum. Methods Phys. Res. B **1**, 481 (1984).
[4] M. Stapelbroek, D. L. Griscom, E. J. Friebele, and G. H. Sigel, Jr., J. Non-Cryst. Solids **32**, 313 (1979).
[5] I. G. Batyrev, B. Tuttle, D. M. Fleetwood, R. D. Schrimpf, L. Tsetseris, and S. T. Pantelides, Phys. Rev. Lett. **100**, 105503 (2008).
[6] L. Skuja, J. Non-Cryst. Solids **239**, 16 (1998).
[7] D. L. Griscom, M. Stapelbroek, and E. J. Friebele, J. Chem. Phys. **78**, 1638 (1983).
[8] D. L. Griscom, in *Structure and Bonding in Noncrystalline Solids*, edited by G. E. Walrafen and A. G. Revesz (Plenum, New York, 1986).
[9] S. Agnello and L. Nuccio, Phys. Rev. B **73**, 115203 (2006).
[10] A. H. Edwards and W. B. Fowler, Phys. Rev. B **26**, 6649 (1982).
[11] L. Nuccio, S. Agnello, and R. Boscaino, J. Phys.: Condens. Matter **20**, 385215 (2008).
[12] S. Agnello, R. Boscaino, M. Cannas, and F. M. Gelardi, Phys. Rev. B **64**, 174423 (2001).
[13] K. M. Davis, A. Agarwal, M. Tomozawa, and K. Hirao, J. Non-Cryst. Solids **203**, 27 (1996).
[14] L. Skuja, B. Güttler, D. Schiel, and A. R. Silin, J. Appl. Phys. **83**, 6106 (1998).
[15] K. M. Davis and M. Tomozawa, J. Non-Cryst. Solids **201**, 177 (1996).
[16] V. G. Plotnichenko, V. O. Sokolov, and E. M. Dianov, J. Non-Cryst. Solids **261**, 186 (2000).
[17] P. W. Atkins, *Physical Chemistry* (Oxford Univeristy Press, New York, 1978).
[18] R. H. Doremus, *Diffusion of Reactive Molecules in Solids and Melts* (John Wiley and Sons, New York, 2002).
[19] L. Nuccio, S. Agnello, and R. Boscaino, Appl. Phys. Lett. **93**, 151906 (2008).
[20] J. W. Lee and M. Tomozawa, J. Non-Cryst. Solids **353**, 4633 (2007).
[21] A. Oehler and M. Tomozawa, J. Non-Cryst. Solids **347**, 211 (2004).
[22] F. Messina and M. Cannas, Phys. Rev. B **72**, 195212 (2005).
[23] K. Kajihara, L. Skuja, M. Hirano, and H. Hosono, Phys. Rev. Lett. **89**, 135507 (2002).
[24] D. L. Griscom, J. Appl. Phys. **58**, 2524 (1985).
[25] F. J. Norton, Nature (London) **191**, 701 (1961).